

PHYSIOLOGICAL MODELLING AND ANALYSIS OF THE PULMONARY MICROCIRCULATION IN SEPTIC PATIENTS

M.A Denai¹, M. Mahfouf¹, O. King¹, J.J. Ross²

¹Dept of Automatic Control & Systems Engineering, University of Sheffield, UK.

²Dept of Anaesthetics, Northern General Hospital, Sheffield, UK.

Abstract: A physiological model integrating a pulsatile cardiovascular system model with a model of the pulmonary capillary fluid exchange based on the Starling's equations is proposed in order to analyse the micro-circulatory physiological alterations which occur during the evolution of sepsis. Sepsis-induced acute lung injury is typically characterized by an increased microvascular permeability and interstitial edema. Pulmonary edema occurs because the capillary filtration capacity increases and the reflection coefficient to proteins decreases causing fluid leak across the capillary barrier. Patients with severe sepsis may develop respiratory failure and hence requiring ventilatory support. These signs represent the clinical expression of the acute respiratory distress syndrome (ARDS) and are associated with high mortality in medical intensive care units (ICU). The proposed model is used to simulate the cardiovascular hemodynamics under these complex pathophysiological conditions. *Copyright © 2006 IFAC*

Keywords: Septic shock, capillary leak, microvascular permeability, pulmonary edema, Starling's force, cardiovascular system.

1. INTRODUCTION

The syndrome of septic shock is characterized by several physiological abnormalities such as: (1) peripheral arteriolar vasodilation which results in low systemic vascular resistance causing hypotension (2) increased heart-rate (2) increased vascular leakage and fluid loss from the intravascular space causing hypovolaemia and (3) myocardial depression with decreased myocardial compliance due to dilated and poorly contractile ventricles (Parillo, 1989; Bridges and Dukes, 2005).

Clinical observations indicate that, in a severe sepsis case, the primary injured target is most often the pulmonary microcirculation. Patients with these clinical complications develop an increased microvascular permeability of the endothelial barrier and interstitial edema. Pulmonary edema diminishes the compliance of the respiratory system and may lead to respiratory failure.

According to Starling's equation, capillary fluid filtration is determined by the hydrostatic and osmotic pressures gradient across the capillary wall. To facilitate gas exchange, the lungs should stay dry

and consequently the balance in Starling's forces is generally in favour of fluid reabsorption. Pulmonary edema occurs when there is fluid accumulation in the interstitial space. This may be caused by an increased capillary pressure (heart failure, arteriolar dilation), increased vascular permeability (sepsis, traumatic injury), decreased plasma oncotic pressure (liver, kidney, nutrition) and eventually lymphatic blockage (lymphedema). This paper is concerned with the analysis of micro-circulatory alterations which are known to occur in the lungs of patients developing severe sepsis. The physiological model used here combines a pulsatile model of the human cardiovascular system with a compartmental model of the pulmonary microvascular exchange. The model is parameterized to simulate the hemodynamic response of a patient under three different stages of sepsis. Quantitative descriptions of the relevant changes in the physiological model parameters are based on the clinician's experiential knowledge.

This paper is organized as follows: First, the physiological model describing the cardiovascular system and the pulmonary microcirculation are presented. The model is then used to simulate the

dynamics of the microvascular exchange of fluid and proteins during the evolution of sepsis. The filtration capacity (K_f) and the reflection coefficient (σ_F) of the lung capillary barrier are gradually increased and decreased respectively to simulate different stages of sepsis.

2. PHYSIOLOGICAL MODEL DESCRIBING THE CARIOVASCULAR SYSTEM AND THE PULMONARY MICROCIRCULATION

2.1 Cardiovascular system model

The cardiovascular system (CVS) model consists of fourteen compartments including the systemic, pulmonary, coronary and cerebral circulations (Denai *et al.*, 2005).

Each compartment consists of a compliant element (C) and a resistance (R) as shown in Fig. 1.

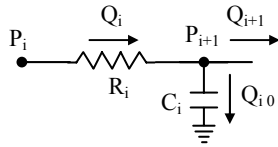


Fig. 1. Electric analog model of a compartment.

The relationships between pressure (P), flow (Q) and volume (V) in a compartment are given as follows:

$$\begin{aligned} P_i &= (V_i - V_{i0}) / C_i \\ Q_i &= (P_i - P_{i+1}) / R_i \\ dV_i / dt &= Q_i - Q_{i+1} \end{aligned} \quad (1)$$

Each ventricle is modelled as time-varying elastance $E(t)$ using the following double Hill equation :

$$E(t) = E_{\min} + E_{\max} \left[\frac{\left(\frac{t_n}{\alpha_1 T} \right)^{n_1}}{1 + \left(\frac{t_n}{\alpha_1 T} \right)^{n_1}} \right] \left[\frac{1}{1 + \left(\frac{t_n}{\alpha_2 T} \right)^{n_2}} \right] \quad (2)$$

The parameters n_1 , n_2 , $\alpha_1 T$ and $\alpha_2 T$ are obtained from experimentally observed elastance curve.

2.2 Mathematical model of the pulmonary microcirculation

The model describing the lung microcirculation consists of three compartments (Bert *et al.*, 1984): circulation, lung tissue and lymph as shown in Fig. 2.

The basic model has been modified so that it can interact with cardiovascular system model.

In the microcirculation, fluid and protein balance is maintained by hydrostatic and oncotic pressures existing on either sides of the capillary barrier.

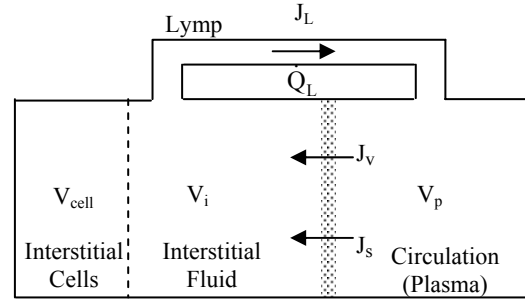


Fig. 2. Compartmental model describing the microvascular exchange.

Filtration takes place at the arteriolar side where hydrostatic pressure is higher than plasma proteins oncotic pressure whereas re-absorption occurs at the venous side as hydrostatic pressure drops along the capillary bed. The lymphatic system regulates this transcapillary exchange by constantly draining fluid and proteins from the interstitium back to the circulation.

The coupling Starling equations describing the transcapillary fluid and protein (k denotes albumin and globulins) exchanges are given as follows

$$\begin{aligned} J_v &= K_f [(P_c - P_i) - \sigma_d (\pi_p - \pi_i)] \\ J_{s,k} &= PS_a (C_{p,k} - C_{AV,k}) + (1 - \sigma_{F,k}) \bar{C}_{s,k} J_v \end{aligned} \quad (3)$$

Where PS_a is the permeability-surface product (the diffuse capacity of the membrane), σ_F is the protein reflection coefficient and $\bar{C}_{s,k} = (C_{p,k} + C_{AV,k})/2$. The total tissue volume of fluid (interstitial and cellular) is the difference between the input and output fluxes such that

$$dV_{\text{tot}} / dt = J_v - J_L \quad (4)$$

The protein concentrations of fluid leaving the tissue and that forming the lymph are assumed identical. Hence the rate of protein transfer through the lymph is expressed as follows

$$dQ_{L,k} / dt = J_L C_{i,k} \quad (5)$$

The tissue protein content is calculated as follows

$$dQ_k / dt = \dot{Q}_{s,k} - \dot{Q}_{L,k} \quad (6)$$

and the tissue fluid volume available to a protein is given by the following expression

$$V_{AV,k} = V_i - V_{E,k} \quad (7)$$

Where $V_i = V_{\text{tot}} - V_{\text{cell}}$ and V_E is the excluded volume which depends on protein size. The protein concentration in lymph which has been approximated

to the protein concentration in the interstitial compartment is given by the following equation:

$$C_{L,k} = C_{i,k} = Q_k / V_i \quad (8)$$

The effective concentration of protein which is responsible for generating the oncotic pressure in the interstitial compartment is based on the tissue volume which is available to proteins and is expressed as follows

$$C_{AV,k} = Q_k / V_{AV,k} \quad (9)$$

This pressure is given as a function of the sum of the concentrations of albumin and globulins (Bert and Pinder, 1984).

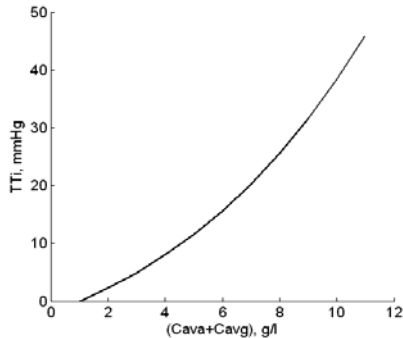


Fig. 3. Oncotic pressure versus plasma protein content: $\pi_i = f(C_{AVa} + C_{AVg})$.

The interstitial compliance is defined by the relationship $P_i = f(V_{tot})$ and is plotted in Fig. 4 (Bert and Pinder, 1984).

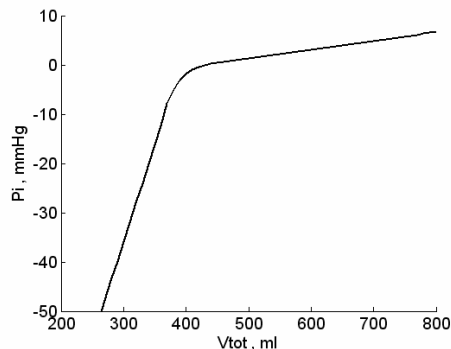


Fig. 4. Interstitial compliance curve: $P_i = f(V_{tot})$.

The plasma protein concentrations are calculated using a similar relationship $\pi_p = f(C_{pa} + C_{pg})$.

Where

$$C_{pa} = \frac{Q_{pa}}{V_p} \quad C_{pg} = \frac{Q_{pg}}{V_p} \quad (10)$$

The plasma volume and protein contents in the plasma are updated using mass balance principle.

$$\frac{dV_p}{dt} = -\frac{dV_{tot}}{dt} \quad (11)$$

$$\frac{dQ_{pa}}{dt} = -\frac{dQ_{ia}}{dt} \quad \frac{dQ_{pg}}{dt} = -\frac{dQ_{ig}}{dt} \quad (12)$$

Finally, the total blood volume in the circulation is $V_{blood} = V_p + V_{rbc}$, V_{rbc} denotes the volume of red blood cells. The proportions of plasma and red blood cells volumes have been set to $V_p = 3400$ ml and $V_{rbc} = 2200$ ml respectively in order to have a total blood

volume in the circulation of 5600 ml. The two models are linked via the pulmonary capillary pressure and through the circulation compartment

3. PHYSIOLOGICAL MODELING OF SEPSIS

Most of septic shock patients undergo alterations in the cardiac function (ventricles contractility (E_{max}) and heart rate (HR)) and peripheral vascular tone (SVR) which directly affect the patient cardiovascular hemodynamics. Furthermore, clinical observations revealed that patients with septic shock have a significantly higher filtration coefficient K_f which may increase up to 6-fold during their stay in ICU (Chris *et al.*, 1998). In addition to increased fluid permeability, microcirculatory dysfunction is also associated with an increased leakage of proteins into the interstitial space (Staub, 1981; Chris *et al.*, 1998). The transcapillary transport of proteins is described by equation (3). The reflection coefficients σ_{Fa} , σ_{Fg} and the permeability-surface product are the main parameters which characterize the protein permeability of the capillary barrier.

The assumed changes in the underlying physiological model parameters are summarized in Tables 1 and 2.

Table 1 Quantitative description of the circulatory parameters in sepsis

	Mild	Moderate	Severe
HR	80	90	110
E_{max}	normal	↓ 30 %	↓ 30 %
SVR	↓ 20 %	↓ 35 %	↓ 50 %

Table 1 Quantitative description of the microvascular parameters in sepsis

	Mild	Moderate	Severe
K_f	normal	↑ 50 %	↑ 100 %
σ_{Fa}	normal	↓ 25 %	↓ 50 %
σ_{Fg}	normal	↓ 20 %	↓ 40 %

4. SIMULATION RESULTS

The cardiovascular system model parameters correspond to a human subject of 75 Kg, a total blood volume of 5600 ml and a heart rate of 75 beats/min have been adapted from (Masuzawa *et al.*, 1992). The values of the parameters corresponding to normal human lungs are listed in the Appendix (Bert and Pinder, 1984). An integration step size of 0.005 sec was used throughout.

4.1 Simulation under normal conditions

All the parameters are set to their nominal values. Fig. 5 shows the simulated left and right ventricle pressures and the aortic and pulmonary pressures related to a normal subject.

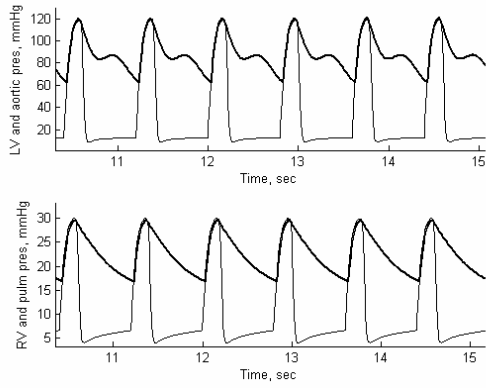


Fig. 5. Simulated left and right ventricles, aortic and pulmonary pressures of a normal subject.

The oncotic model describing the dynamics of the pulmonary microcirculation requires initial values for the extravascular volume and proteins contents which are set to $V_{tot} = 300$ ml, $Q_a = 5.93$ g and $Q_g = 2.48$ g respectively. Fig. 6 and 7 show the transient response of the volume, oncotic pressure, hydrostatic pressure and protein concentration in the plasma and the interstitial space respectively.

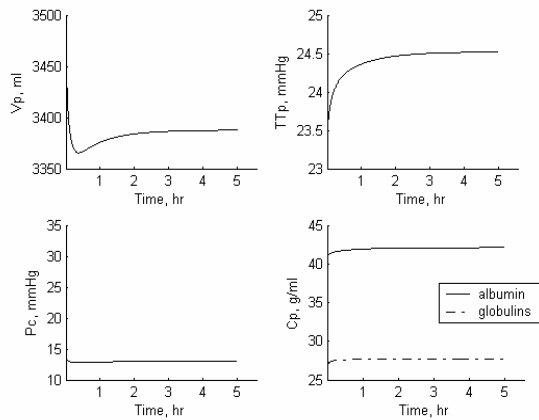


Fig. 6. Transient responses of V_p , π_p , P_c and C_p .

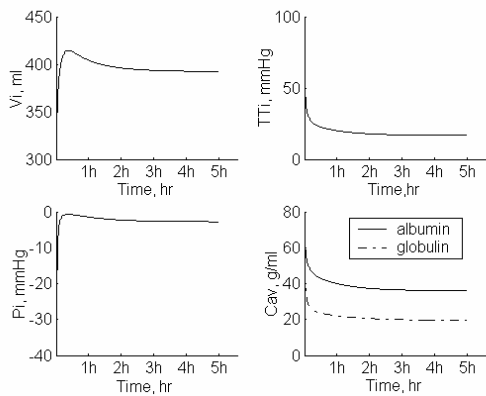


Fig. 7. Transient responses of V_i , π_i , P_i and C_{av} .

The steady-state normal values of the parameters are listed in Table 3. All the values compare favourably

with published data for human lungs (Bert and Pinder, 1984; Roselli *et al.*, 1984).

Table 3 Steady-state oncotic model parameter values

$\pi_p = 25$ mmHg	$\pi_i = 16.8$ mmHg
$C_{pa} = 42$ g/ml	$C_{ava} = 36.5$ g/ml
$C_{pg} = 27.8$ g/ml	$C_{avg} = 20$ g/ml
$P_c = 13$ mmHg	$P_i = -2.8$ mmHg
$V_p = 3390$ ml	$V_i = 392$ ml

4.2 Simulation under septic conditions

The physiological model parameters are varied according to Fig. 8 to simulate the hemodynamic alterations in a patient going through the three different stages of sepsis. Similar patterns are applied to the pulmonary oncotic model parameters K_f , σ_{Fa} and σ_{Fg} . All these parameters changes are allowed to occur simultaneously throughout the assumed septic stages.

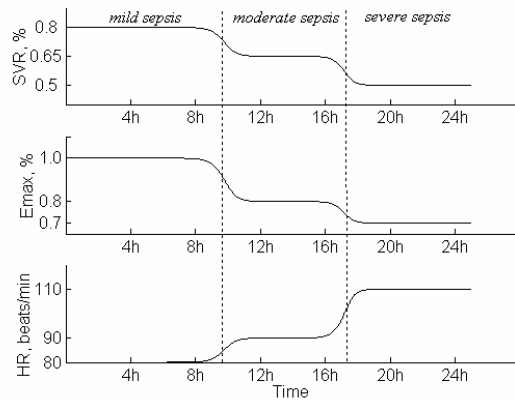


Fig. 8. Simulated parameters changes under sepsis conditions.

The hemodynamic responses to these pathophysiological conditions are shown in Fig. 9. There is a fall in the circulating blood volume due to the increasing permeability of the capillary barrier. This contributes to the marked increase in the cardiac output (CO). A decrease in arteriolar and venous tones results in a systemic hypotension and increased venous capacity respectively. In reality, these alterations may vary at different vascular beds, which lead to a maldistribution of blood flow in the circulation and subsequent cascaded organs dysfunction at a later stage.

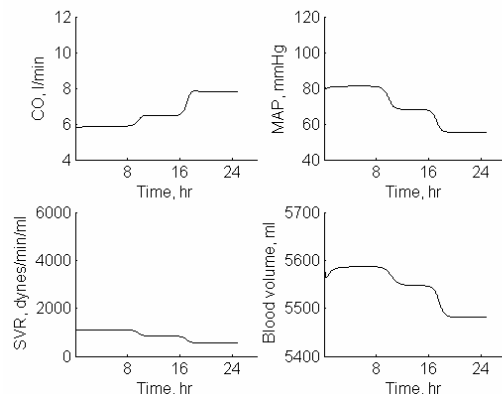


Fig. 9. Cardiovascular hemodynamic responses under sepsis.

The steady-state hemodynamic data for simulated non-septic and septic patients are listed in Table 4.

Table 4 Hemodynamic data for simulated non-septic and septic patients.

		Non-septic	Septic		
			Mild	Moderate	Severe
CO	l/min	5.2	5.8	6.5	7.8
MAP	mmHg	94.0	81.0	68.0	55.4
HR	beats/min	75.0	80.0	90.0	110.0
MPAP	mmHg	22.4	23.8	23.8	23.5
CVP	mmHg	7.1	7.7	8.5	8.9
PCP	mmHg	13.0	13.4	13.7	13.6
SVR	dyn.s.cm ⁻⁵	1409.5	1105.3	842.9	566.9

Microvascular changes in the pulmonary circulation are shown in Fig. 10 and 11. As the capillary barrier becomes more permeable to plasma fluid and proteins, hydrostatic and oncotic pressures in the interstitial compartment are expected to increase. The gained fluid volume and proteins in the interstitial space contribute to an expansion of the extracellular volume (Fig. 11). There is a slight increase in the pulmonary capillary hydrostatic pressure due to the increase in the cardiac output.

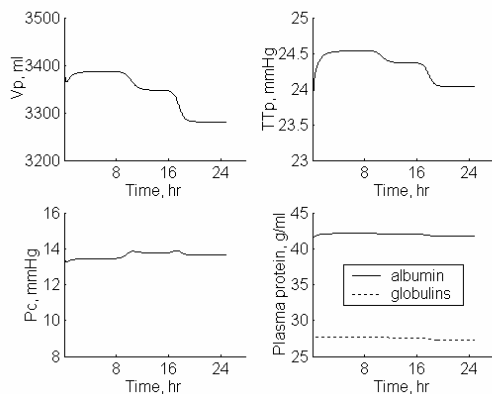


Fig. 10. Transient responses of V_p , π_p , P_c and C_p under sepsis.

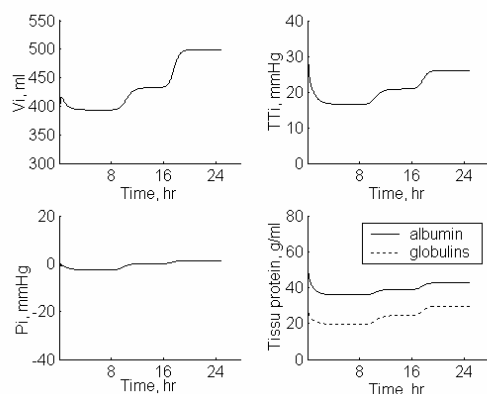


Fig. 11. Transient responses of V_i , π_i , P_i and C_{av} under sepsis.

Lung fluid balance is determined by the net fluid flow ($J_V - J_L$) which should be equal to zero so that a tissue fluid volume is maintained constant. As filtration flow J_V increases, the flow of the lung's lymphatic system J_L will increase to conserve a zero net fluid flow. As shown in Fig. 12, there is a time

lag between J_V and J_L which causes fluid to accumulate in the lungs (Drake *et al.*, 1987). However, if the filtration rate exceeds the transport capacity of the lymphatic system, fluid accumulation in the interstitial compartment is increased and leads to pulmonary edema.

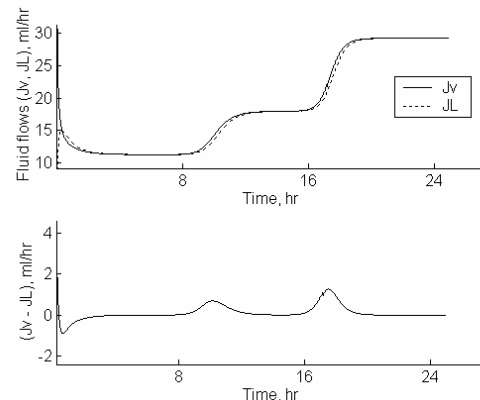


Fig. 12. Inter-compartmental fluid flows

4.3 Severe sepsis with lymphedema

Other physiological conditions can be simulated such as changes in lymph flow characteristics to characterize different forms of lymphedema. The lymphatic pumping capacity is modulated by V_{tot} through the linear relationship given in the Appendix. Fig. 13 shows the effects of decreasing the lymphatic flow by 10% and 20% respectively. The model parameters are those related to severe sepsis conditions. There is an increased interstitial volume expansion due to the decreased lymphatic pumping capacity and this contributes to edema accumulation.

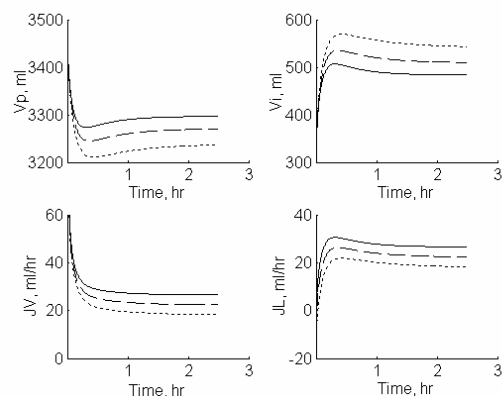


Fig. 13 Effect of decreased lymph flow : normal (solid), -10% (dashed), -20% (dotted)

5. CONCLUSIONS

The modelling and simulation studies presented in this paper aimed at analyzing the mechanisms which affect the pulmonary microcirculation during different stage of sepsis. The physiological model structure proposed herein represents a useful approach for understanding sepsis-induced organ dysfunctions and their effects on the cardiovascular hemodynamics.

The present investigation concentrated on those factors characterizing the permeability of the lung microcirculation during the evolution of severe sepsis. The model simulated successfully the contribution of these factors to the development of clinical symptoms of severe sepsis such as capillary leakage, pulmonary edema and hypovolemia. Data collection from real patients in cardiac ICU is under way which will help tune the model parameters and validate its implementation into a decision support system for the management of septic shock patients.

ACKNOWLEDGEMENTS

The authors gratefully acknowledge the financial support for this project from the UK Engineering and Physical Sciences Research Council (EPSRC) under Grant GR/S94636/1.

APPENDIX

Nomenclature

CO	cardiac output
HR	heart-rate
MAP	mean arterial pressure
MPAP	mean pulmonary arterial pressure
CVP	central venous pressure
PCP	pulmonary capillary pressure
SVR	systemic vascular resistance
P_c	capillary hydrostatic pressure
P_i	interstitial hydrostatic pressure
π_c	capillary oncotic pressure
π_i	interstitial oncotic pressure
J_v	fluid flux from plasma into tissue (ml/hr)
J_s	protein flux from plasma into tissue(g/hr)
J_L	lymph flow (ml/hr)
V_{tot}	total extravascular volume (ml)
V_i	interstitial fluid volume (ml)
V_{AV}	interstitial volume available to protein (ml)
V_E	excluded volume (ml)
V_{cell}	cellular volume (ml)
Q	protein content of interstitial fluid (g)
dQ/dt	rate of protein transfer (g/hr)
Q_L	protein flux from tissue to lymph
C_p	protein concentration in plasma
C_i	protein concentration in tissue
C_{AV}	protein concentration in tissue based on V_{AV}
C_L	protein concentration in lymph
K_f	fluid filtration coefficient (ml/hr.mmHg)
σ_d	fluid reflection coefficient
σ_F	protein reflection coefficient
PS	permeability surface area

Parameter values for normal human lungs.

K_f	1.12 ml/hr.mmHg
σ_d	0.75
V_{cell}	150 ml
J_L	$0.17V_{tot} - 55.6$
PS_a	3.0 ml/hr
σ_{Fa}	0.4
V_{Ea}	73.5 ml
PS_g	1.0 ml/hr
σ_{Fg}	0.6
V_{Eg}	115.5 ml

REFERENCES

- Auckland K., R.K. Reed (1993), Interstitial-lymphatic mechanisms in the control of extracellular fluid volume, *Physiol Rev*, **73**, 1-78.
- Bert, J.L., K.L. Pinder (1984). Pulmonary microvascular exchange: An analog computer simulation, *Microvascular Research*, **27**, 51-70.
- Bridges E.J., M.S. Dukes, Cardiovascular aspects of septic shock: Pathophysiology, monitoring and treatment, *Critical Care Nurs*, **25**, 2005, 14-40.
- Chris E., J. Gamble, L.B. Gartside and W.J. Kox (1998). Increased microvascular water permeability in patients with septic shock, assessed with venous congestion plethysmography (VCP), *Intensive Care Med*. **24**, 18-27.
- Denai M.A., M. Mahfouf, J.J. Ross (2005). A physiological model describing dobutamine interaction with septic patients: A simulation study, Proceedings of 3rd European Medical and Biological Engineering Conference (EMBEC'05), 20-25 Nov. 2005, Prague.
- Drake R.E., G.A. Laine, S.J. Allen, J. Katz and J.C. Gable (1987), A model of the lung interstitial-lymphatic system, *Microvascular Research*, **34**, 96-107.
- Masuzawa T., Y. Fukui and N.T. Smith (1992). Cardiovascular simulation using a multiple modeling method on a digital computer – simulation of interaction between the cardiovascular system and angiotensin II, *J. of Clin. Monitoring*, **8**, 50-58.
- Parillo, J.E. (1989). The cardiovascular pathophysiology of sepsis, *Ann. Rev. Med.*, **40**, 469-85.
- Roselli, R., R.E. Parker and T.R. Harris (1984), A model of unsteady-state transvascular fluid and protein transport in the lung, *J. Appl. Physiol*, **56**, 1389-1402.
- Staub, N.C. (1981). Pulmonary oedema due to increased microvascular permeability, *Ann. Rev. Med.*, **32**, 291-312.
- Wiederhielm, C.A. (1979). Dynamics of capillary fluid exchange: A nonlinear computer simulation, *Microvascular Research*, **18**, 48-82.
- Xie, S.L., R.K. Reed, B.D. Bowen and J.L. Bert (1995). A model of human microvascular exchange, *Microvascular Research*, **49**, 141-162.